Electronic Supplementary Material

Decoration of $CdMoO_4$ micron polyhedron with Pt nanoparticle and their enhanced photocatalytic performance in N_2 fixation and water purification

Xujie Ren[1], Junfeng Wang[1], Shude Yuan[1], Chunran Zhao[1], Lin Yue[3], Zhihao Zeng[3], Yiming He (✉)[1,2]

1 Department of Materials Science and Engineering, Zhejiang Normal University, Jinhua 321004, China

2 Key Laboratory of Solid State Optoelectronic Devices of Zhejiang province, Zhejiang Normal University, Jinhua 321004, China

3 Key Laboratory of the Ministry of Education for Advanced Catalysis Materials, College of Chemistry and Materials Science, Zhejiang Normal University, Jinhua 321004, China

E-mail: hym@zjnu.cn

1. Photocatalytic N_2 fixation reaction

The photocatalytic nitrogen fixation experiments were conducted in a self-built photochemical reactor. A 300W Xe lamp (PLS-SXE300C, Beijing ProfectLight Co. Ltd., China) was used as the simulated sunlight source. 0.1 g of solid catalyst was added into a 100 mL methanol solution (containing 5 mL methanol and 95 mL deionized water) and stirred for 1 h in the dark to ensure an adsorption–desorption equilibrium. During light exposure, 7 mL of the liquid was extracted from the solution every one-hour interval for ammonia detection. The sample solution was centrifuged to obtain the supernatant, and then 30 μL of sodium tartrate and 30 μL of Nessler's reagent were added successively. After 12 min of reaction, the ammonia concentration was analyzed by measuring the absorbance at 420 nm with a UV-vis spectrophotometer. The photocatalytic N_2 fixation in the presence of different scavengers was conducted similarly, except that the scavenger was changed. For the reaction performed in the presence of N_2, the bubbling N_2 flow rate was controlled to 50 mL min^{-1}. For the reaction under vacuum, the reactor was replaced with a closed quartz reactor. After the reaction solution and catalyst were added, the air in the reactor was evacuated, and the relative pressure to the outside world was maintained at -97kPa (the actual pressure was about 4.3kPa).

2. Photocatalytic tetracycline (TC) degradation reaction

The photocatalytic activities of Pt/$CdMoO_4$ photocatalysts were evaluated by measuring the degradation rate of TC in solution at room temperature under simulated sunlight. Briefly, 0.1 g of each photocatalyst was dispersed into 100 mL of TC solution (10 ppm) under magnetic stirring. After continuous stirring for 1 h, an adsorption-desorption equilibrium was established between the

photocatalyst and TC solution. During illumination, 4 mL of the solution was collected at 15-minute intervals. The collected samples were centrifuged to remove the photocatalyst, and the supernatant was analyzed via a UV-vis spectrophotometer (Beijing Purkinje, TU-1950) to determine the TC content.

The examination experiment process of reactive species was similar to the photodegradation experiment. A quantity of scavengers (potassium iodide, ascorbic acid, β-carotene, and isopropyl alcohol) was introduced into the TC solution prior to addition of the catalyst. The concentration of scavengers was controlled to be 0.01 μmol/L according to the previous studies.

3. Determination of NH_3 content by the NMR method

After 5-hour photocatalytic reaction, the NH_4^+ content was quantitatively determined by ^1H nuclear magnetic resonance (NMR, 600 MHz, Bruker AV600) with external standards, taking maleic acid ($C_4H_4O_4$) as a reference. To create the calibration curve, a series of NH_4^+ solutions with known concentration were prepared in 0.01 M HCl as standards. Next, 24.5 mL of the NH_4^+ standard solution was mixed with 0.5 mL maleic acid (25 μg/mL). The mixture was then concentrated to approximately 1 mL and identified using ^1H NMR spectroscopy (50 μL deuterium oxide (D_2O) was added in 0.45 mL concentrated solution before NMR detection). The calibration was achieved using the peak area ratio between NH_4^+ and tris-maleate because the NH_4^+ concentration and the area ratio are positively correlated. Similarly, the NH_4^+ concentration after photocatalytic reaction was quantitatively determined using this method.

4. Characterizations of $Pt/CdMoO_4$ photocatalysts

X-ray diffraction (XRD) analysis was performed on a D8 Advance (BRUKER AXS GMBH, Germany) X-ray diffractometer using Cu Kα radiation (40 kV/40 mA). The Raman spectra of the $Pt/CdMoO_4$ catalysts were recorded on a RM1000 spectrometer (Renishaw) via an excitation source of an Ar ion laser (514.5 nm). Scanning electron microscopy (SEM) was carried out on a Field emission scanning electron microscope (Hitachi S-4800) with the accelerating voltage of 5 kV. Transmission electron microscopy (TEM) was employed on a JEM-2010F transmission electron microscope via the accelerating voltage of 200 kV. The X-ray photoelectron spectroscopy (XPS) spectra of the catalysts were obtained via using a Thermo Scientific ESCALAB 250Xi Microprobe instrument using Al-Kα as a ray source. The C 1s signal was adjusted in the location of 284.6 eV. UV-visible diffuse reflection spectroscopy (DRS) was actualized on a UV-visible spectrophotometer (Agilent Cary5000) and the reference sample was $BaSO_4$. A CHI 660E electrochemical workstation with a standard three-electrode cell was employed to perform the photocurrent (PC) responses, electrochemical impedance spectroscopy (EIS), and Mott-Schottky measurements. The test was operated at room temperature. The photocatalyst, Ag/AgCl (saturated KCl), and a Pt wire were used as the working electrode, the reference electrode, and the counter electrode, respectively. The coated area of the photocatalyst on the ITO glass was 1×1 cm and Na_2SO_4 (0.5 M) aqueous solution was used as the electrolyte. For PC measurement, a 300 W Xe lamp was served as the light source. photoluminescence (PL) spectra of the photocatalyst were recorded on an FLS-920 fluorescence spectrometer manufactured by Edinburgh-Instrument, UK.

The X-band electron spin-resonance (ESR) spectra were recorded at room temperature using a Bruker model ESR JES-FA200 spectrometer. The sample for ESR measurement was prepared by adding 5 μL 5,5′-dimethyl-1-pirroline-N-oxide (DMPO) to a 50 μL of 1 g/L catalyst aqueous

solution or toluene solution to detect $\cdot O_2^-$ radicals, respectively. The photocatalysts were irradiated with the aforementioned visible light for 5 min. The ESR measurement was performed immediately after the illumination. The hole detection experiment was implemented by the similar process. Only DMPO was replaced by 2,2,6,6-tetramethylpiperidine N-oxide (TEMPO).

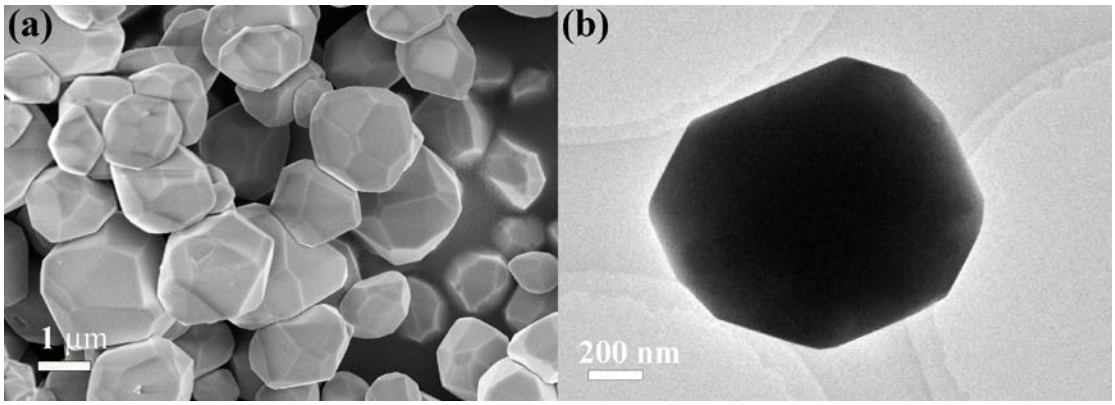

Figure S1 SEM (a) and TEM (b) images of $CdMoO_4$.

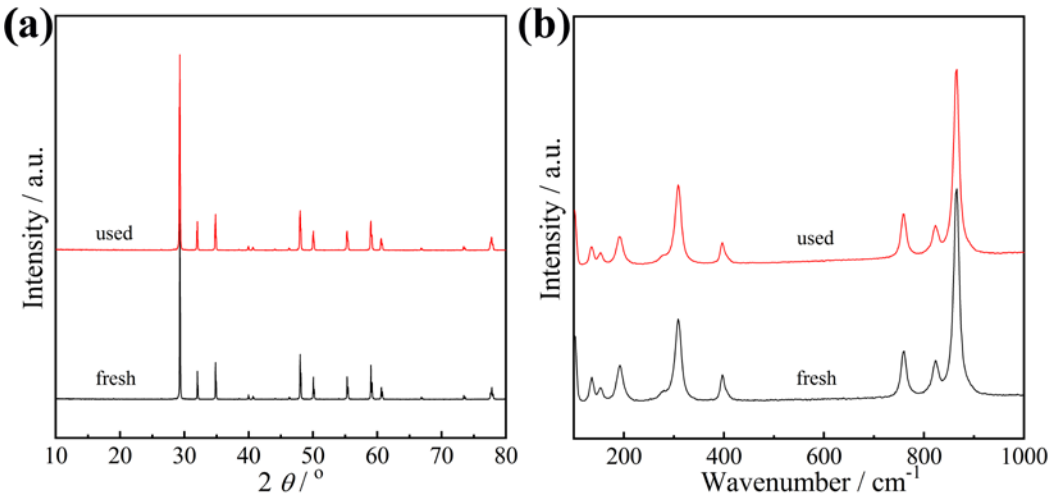

Figure S2 XRD patterns (a) and Raman spectra (b) of 0.6%Pt/$CdMoO_4$ composite before and after the PNF reaction.

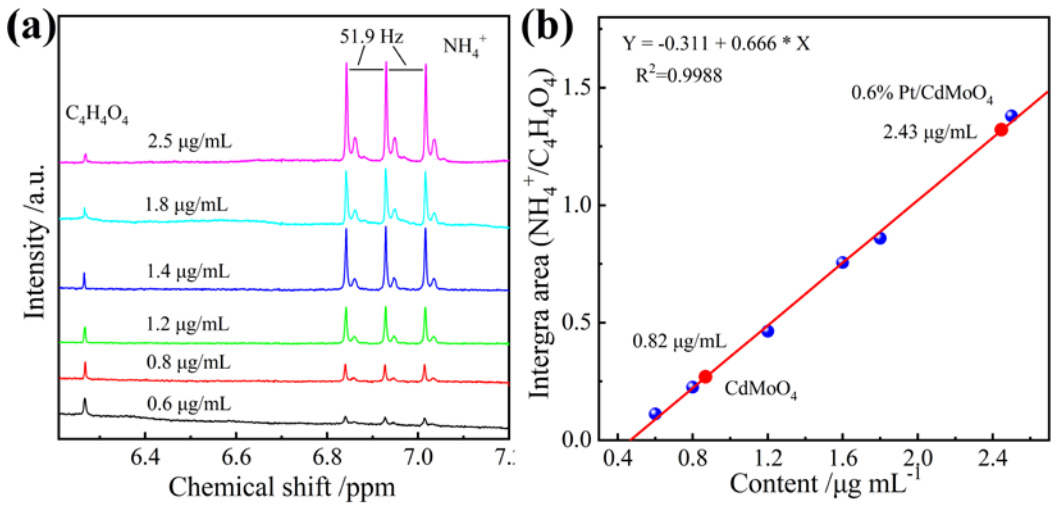

Figure S3 ^{1}H NMR spectra (600 MHz) of various $^{14}NH_4^+$ solutions (a) and the standard curve line obtained via the external standard method (b).

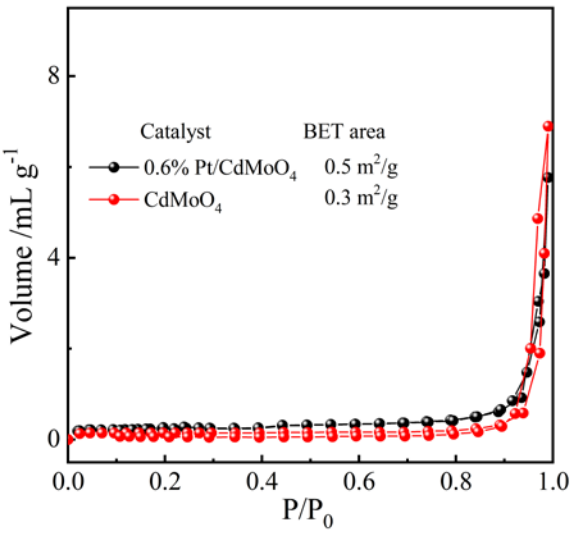

Figure S4 N_2 adsorption-desorption isotherms of $CdMoO_4$ and 0.6% Pt/$CdMoO_4$ composite

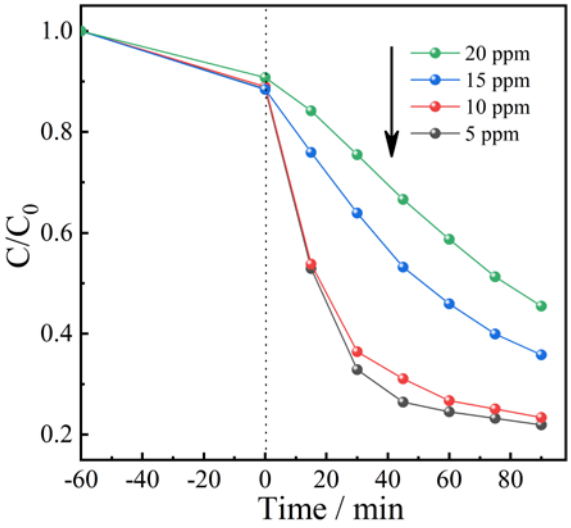

Figure S5 Effect of TC content on the photocatalytic activity of 0.6% Pt/$CdMoO_4$ catalyst.

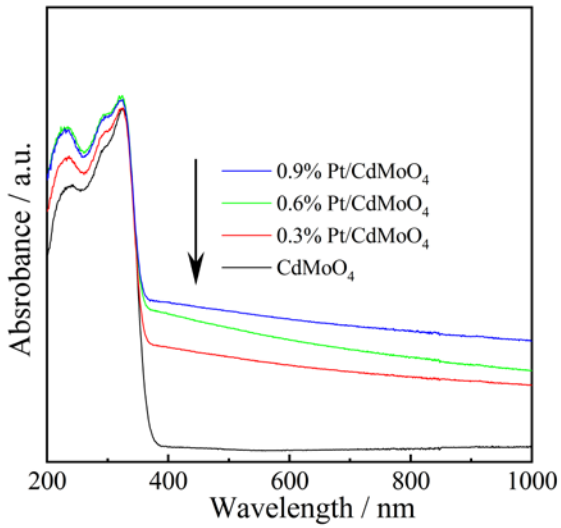

Figure S6 DRS spectra of Pt/$CdMoO_4$ catalyst with different Pt content.

Table S1 Calculated lattice constants of $CdMoO_4$ and 0.6% Pt/$CdMoO_4$ catalysts

Catalyst	a /Å	b/ Å	c/ Å	V/ $Å^3$	[a]FWHM	Crystalline size/nm
$CdMoO_4$	5.1505	5.1505	11.1889	296.82	0.105	91.5
0.6% Pt/$CdMoO_4$	5.1492	5.1492	11.1864	296.59	0.103	93.2

a Note: the full width at half maximum of the diffraction peak at 2θ=29.2 °

Table S2 Summary of some metal molybdate photocatalysts for the N_2 reduction to NH_3

Catalyst	Nitrogen source	Sacrificial agent	NH_3 generation rate/μmol·$L^{-1}g^{-1}·h^{-1}$		Light source	Ref.
			Nessler method	NMR method		
Br-Bi_2MoO_6	N_2	CH_3OH	400	-	300W Xe	[1]
Gd-Bi_2MoO_6	N_2	CH_3OH	300	-	300W Xe	[2]
Vo-Bi_2MoO_6	N_2	CH_3OH	800	-	300W Xe	[3]
$Bi_3FeMo_2O_{12}$	N_2	CH_3OH	1156	-	450W Hg	[4]
Co-Bi_2MoO_6	N_2	CH_3OH	130	-	300W Xe	[5]
Cu-Bi_2MoO_6	air	CH_3OH	302	265	300W Xe	[6]
Fe-$SrMoO_4$	N_2	CH_3OH	93.1	-	300W Xe	[7]
CN/$ZnMoO_4$	N_2	CH_3CH_2OH	3120	-	500W Xe	[8]
Bi-$CdMoO_4$	Air	CH_3OH	590	272	300W Xe	[9]
Pt/$CdMoO_4$	Air	CH_3OH	443	286	300W Xe	This work

Table S3 Comparison of photocatalytic TC degradation efficiency among various heterostructured catalysts

Photocatalyst	TC content	Light source	Reaction time	Degradation efficiency	Ref.
MoO_3/g-C_3N_4	20 mg/L	350 W Xe lamp	90min	43.2%	[10]
CDs/MoO_3/g-C_3N_4	20 mg/L	350 W Xe lamp	90min	88.4%	[10]
Ag/Bi_3TaO_7	10 mg/L	250 W Xe lamp	90min	85.4%	[11]
$Zn_{1-x}Cd_xS$	40 mg/L	300 W Xe lamp	70min	79.0%	[12]
N-g-C_3N_4	10 mg/L	30 W LED	60 min	60%	[13]
Bi/$BiVO_4$	10 mg/L	250 W Xe lamp	60 min	74.7%	[14]
C-ZnO/A-CN	20 mg/L	300 W Xe lamp	100 min	86.5%	[15]
$BiOIO_3$/BiOBr	20 mg/L	12 W LED lamp	80 min	74.9%	[16]
CDs/H-CN	20 mg/L	300 W Xe lamp	120 min	86%	[17]
$MoSe_2$/AgBr	10 mg/L	300 W Xe lamp	90 min	75.7%	[18]
Pt/$CdMoO_4$	20mg/L	300 W Xe lamp	90 min	77.0%	This work

References:

1. G.A. Wang, T.T. Huo, Q.H. Deng, F. Yu, Y.G. Xia, H.P. Li, W.G. Hou, Surface-layer bromine doping enhanced generation of surface oxygen vacancies in bismuth molybdate for efficient photocatalytic nitrogen fixation, Applied Catalysis B: Environmental 310 (2022) 121319

2. H.D. Li, H. Zhao, C.P. Li, B.Q. Li, B.R. Tao, S.N. Gu, G.F. Wang, H.X. Chang, Redox regulation of photocatalytic nitrogen reduction reaction by gadolinium doping in two-dimensional bismuth molybdate nanosheets, Applied Surface Science 600 (2022) 154105
3. G. Li, W.Y. Yang, S. Gao, Q.Q. Shen, J.B. Xue, K.X. Chen, Q. Li, Creation of rich oxygen vacancies in bismuth molybdate nanosheets to boost the photocatalytic nitrogen fixation performance under visible light illumination, Chemical Engineering Journal 404 (2021) 127115
4. B.T. Liu, A.S. Yasin, T. Musho, J. Bright, H.B. Tang, L. Huang, N.Q. Wu, Visible-Light Bismuth Iron Molybdate Photocatalyst for Artificial Nitrogen Fixation, Journal of The Electrochemical Society 166 (2019) H3091–H3096
5. Z.Y. Liu, X.M. Li, S.D. Su, W.M. Ding, L.H. Meng, Y.Y. Wang, M.Y. Tan, M. Luo, Enhancing photocatalytic nitrogen fixation performance of Co-doped bismuth molybdate through band engineering tuning, Applied Surface Science 611 (2023) 155627
6. J.F. Wang, C.R. Zhao, S.D. Yuan, X.J. Li, J.Y. Zhang, X. Hu, H.J. Lin, Y. Wu, Y.M. He, One-step fabrication of Cu-doped Bi_2MoO_6 microflower for enhancing performance in photocatalytic nitrogen fixation, Journal of Colloid and Interface Science 638 (2023) 427-438
7. J.Y. Luo, X.X. Bai, Q. Li, X. Yu, C.Y. Li, Z.N. Wang, W.W. Wu, Y.P. Liang, Z.H. Zhao, H. Liu, Band structure engineering of bioinspired Fe doped $SrMoO_4$ for enhanced photocatalytic nitrogen reduction performance, Nano Energy 66 (2019) 104187
8. M. Mousavi, S. Moradian, P. Pourhakkak, G.K. Zhang, M.M.Habibi, M. Madadi, J.B. Ghasemi, Fabrication of S-scheme heterojunction g-C_3N_4- nanosheet/$ZnMoO_4$ nanocomposite with high efficiency in photocatalytic N_2 fixation and Cr(VI) detoxification, Journal of Material Science 57 (2022) 9145–9163
9. J.F. Wang, L.F. Guan, S.D. Yuan, J.Y. Zhang, C.R. Zhao, X. Hu, B.T. Teng, Y. Wu, Y.M. He, Greatly boosted photocatalytic N_2-to-NH_3 conversion by bismuth doping in $CdMoO_4$: Band structure engineering and N_2 adsorption modification, Separation and Purification Technology, 314 (2023) 123554
10. Z.J. Xie, Y.P. Feng, F.L. Wang, D.N. Chen, Q.X. Zhang, Y.Q. Zeng, W.Y. Lv, G.G. Liu, Construction of carbon dots modified MoO_3/g-C_3N_4 Z-scheme photocatalyst with enhanced visible-light photocatalytic activity for the degradation of tetracycline, Applied Catalysis B: Environmental 229 (2018) 96–104
11. B.F. Luo, D.B. Xu, D. Li, G.L. Wu, M.M. Wu, W.D. Shi, M. Chen, Fabrication of a Ag/Bi_3TaO_7 Plasmonic Photocatalyst with Enhanced Photocatalytic Activity for Degradation of Tetracycline, ACS Applied Material Interfaces 7 (2015) 17061–17069
12. J.X. Tan, G.Q. Wei, Z. Wang, H. Su, L.T. Liu, C.H. Li, J.J. Bian, Application of $Zn_{1-x}Cd_xS$ Photocatalyst for Degradation of 2-CP and TC, Catalytic Mechanism, Catalysts 12 (2022) 1100
13. H.R. Sun, F. Guo, J.J. Pan, W. Huang, K. Wang, W.L. Shi, One-pot thermal polymerization route to prepare N-deficient modified g-C_3N_4 for the degradation of tetracycline by the synergistic effect of photocatalysis and persulfate-based advanced oxidation process, Chemical Engineering Journal 406 (2021) 126844
14. N.J. Kang, D.B. Xu, W.D. Shi, Synthesis plasmonic Bi/$BiVO_4$ photocatalysts with enhanced photocatalytic activity for degradation of tetracycline (TC), Chinese Journal of Chemical Engineering 27 (2019) 3053–3059

15. X.Y. Huang, X.Y. Zhang, K.X. Zhang, X.G. Xue, J. Xiong, Y. Huang, D.D. Zhang, J. Zhang, Z.L. Zhang, F.P. Yan, Defect-mediated Z-scheme carriers' dynamics of C-ZnO/A-CN toward highly enhanced photocatalytic TC degradation, Journal of Alloys and Compounds 877 (2021) 160321
16. X. Kuang, M. Fu, H. Kang, P. Lu, J.W. Bai, Y. Yang, S.X. Gao, A $BiOIO_3$/BiOBr n-n heterojunction was constructed to enhance the photocatalytic degradation of TC, Optical Materials 138 (2023) 113690
17. W.L. Shi, S. Yang, H.R. Sun, J.B. Wang, X. Lin, F. Guo, J.Y. Shi, Carbon dots anchored high-crystalline g-C_3N_4 as a metal-free composite photocatalyst for boosted photocatalytic degradation of tetracycline under visible light, Journal of Material Science 56 (2021) 2226–2240
18. J.H. Yang, J.L. Sun, S. Chen, D.Q. Lan, Z.H. Li, Z.J. Li, J.W. Wei, Z.B. Yu, H.X. Zhu, S.F. Wang, Y.P. Hou, S-scheme 1 T phase $MoSe_2$/AgBr heterojunction toward antibiotic degradation: Photocatalytic mechanism, degradation pathways, and intermediates toxicity evaluation, Separation and Purification Technology 290 (2022) 120881